Inorganic Chemistry
Communication

Origin of the Unusual Stability of B_{12} and B_{13}^{+} Clusters

Boggavarapu Kiran,*[†] G. Gopa Kumar,[‡] Minh T. Nguyen,[‡] Anil K. Kandalam,[§] and Puru Jena[⊥]

[†]*Department of Chemistry, McNeese State University, Lake Charles, Louisiana 70609,* [‡]*Department of Chemistry, Katholieke Universiteit Leuven, 200-F, B-3001 Leuven, Belgium,* [§]*Department of Physics, McNeese State University, Lake Charles, Louisiana 70609, and* [⊥]*Department of Physics, Virginia Commonwealth University, Richmond, Virginia 23284*

A novel way to analyze the boron clusters is proposed in which the cluster is partitioned as inner and outer rings. Fragment molecular orbital analysis, based on this fragmentation, reveals that the delocalized valence electrons in B_{12} and B_{13}^{+} clusters can be trifurcated as $6\pi-6\sigma_{delo}-6\sigma_{3\text{-ring}}$, leading to triple aromaticity, which is unique to these clusters.

Boron never ceases to surprise. From simple hydrides to complex solid-state structures, boron offers a rich variety of bonding features that defy conventional thinking. For example, a polyhedral or three-dimensional structure, especially B_{12} icosahedra, is a recurring structural pattern in most of the boron compounds.[1] In contrast, bare boron clusters adopt planar, quasi-planar, or tubular structures depending on the size of the cluster.[2,3]

Among the small B clusters, B_{12} and B_{13}^{+} are particularly unique. In one of the earliest experimental studies, Anderson and co-workers observed an unusually high intense peak for B_{13}^{+} in the mass spectrum of cationic boron clusters.[4] In subsequent studies, the group further noticed an unusual reactivity pattern for B_{13}^{+}, namely, a high threshold for oxidation,[5] and low reactivity[6] with D_2O compared to the similarly sized clusters. In addition, dissociation of the B_{13}^{+} cluster to B_{12} and B^{+} is more facile compared to other B_n^{+} clusters, suggesting that B_{12} is very stable. This is consistent with the earlier theoretical prediction[7] that most stable clusters, conventionally referred to as magic clusters, are always the preferred byproducts in the dissociation of a parent cluster. Anion photoelectron spectroscopic studies corroborate this finding: B_{12}^{-} exhibits the *least* intense peak in the B_n^{-} mass spectra, and the neutral B_{12} has the *largest* HOMO−LUMO (H−L) gap (∼2.0 eV).[8] In comparison, the H−L gap of C_{60} is ∼1.68 eV.[9]

In order to account for these observations, earlier theoretical studies[3,8,10−12] have focused on π-electron delocalization as an important component for the planarity and stability of B_{12} and B_{13}^{+}, where 6π electrons occupy orbitals akin to the benzene π levels. However, this cannot be the complete story because B_{10} also has benzene-like 6π electrons but its H−L gap (∼1.0 eV) is much smaller than that of B_{12}. In addition, B_{14} has 8π electrons[8] but has a H−L gap similar to that of B_{10}. Thus, studies based on π electrons alone cannot account for all of these observations.

In this Communication, we show that the extraordinary kinetic stability of B_{12} and B_{13}^{+} is related to the *triply* aromatic nature of these clusters. We further show that the H−L gaps are, in fact, governed by the size and nature of the interaction between the outer and inner rings of the planar clusters. The computational details are given in the Supporting Information.

First, we focus on the nature of the bonding in B_{12}. In agreement with earlier studies,[2a,8] we found that neutral B_{12} adopts a C_{3v} ground-state geometry with an outer nine-membered (B_9) ring and an inner B_3 ring [$B_9(B_3)$] (Figure 1). The inner ring is slightly out of the plane, and the planar D_{3h} structure is only 0.12 eV higher in energy. Inspection of the bond-length variations in B_{12} provides preliminary hints about the nature of electron delocalization. The B−B bond lengths in the B_9 ring (1.55 and 1.61 Å) are shorter than the B−B distance in the B_3 ring (1.65 Å), which is further shorter than the B−B distances (1.68 and 1.81 Å) between the B_9 and B_3 rings. To put these distances into

*To whom correspondence should be addressed. E-mail: kiran@mcneese.edu.

(1) (a) Jemmis, E. D.; Prasad, D. L. V. K. *J. Solid State Chem.* **2006**, *179*, 796–802. (b) Jemmis, E. D.; Balakrishnarajan, M. M. *Bull. Mater. Sci.* **1999**, *22*, 863–867. (c) Perkins, C. L.; Trenary, M.; Tanaka, T. *Phys. Rev. Lett.* **1996**, *77*, 4772.

(2) (a) Boustani, I. *Chem. Phys. Lett.* **1995**, *240*, 135–140. (b) Ricca, A.; Bauschlicher, C. W. *Chem. Phys.* **1996**, *208*, 233–242. (c) Boustani, I. *Surf. Sci.* **1997**, *370*, 355. (d) Boustani, I. *Phys. Rev. B* **1997**, *55*, 16426.

(3) Fowler, J. E.; Ugalde, J. M. *J. Phys. Chem. A* **2000**, *104*, 397–403.

(4) Hanley, L.; Whitten, J. L.; Anderson, S. L. *J. Phys. Chem.* **1988**, *92*, 5803–5812.

(5) Hanley, L.; Anderson, S. L. *J. Chem. Phys.* **1988**, *89*(5), 2848–2860.

(6) Hintz, P. A.; Ruatta, S. A.; Anderson, S. L. *J. Chem. Phys.* **1990**, *92*(1), 292–303.

(7) Rao, B. K.; Jena, P.; Manninen, M.; Nieminen, R. *Phys. Rev. Lett.* **1987**, *58*, 1188.

(8) Zhai, H. J.; Kiran, B.; Li, J.; Wang, L. S. *Nat. Mater.* **2003**, *2*, 827–833.

(9) Wang, X. B.; Ding, C. F.; Wang, L. S. *J. Chem. Phys.* **1999**, *110*, 8217–8220.

(10) Aihara, J. *J. Phys. Chem. A* **2001**, *105*, 5486–5489.

(11) Lau, K. C.; Deshpande, M. D.; Pandey, R. *Int. J. Quantum Chem.* **2005**, *102*, 656.

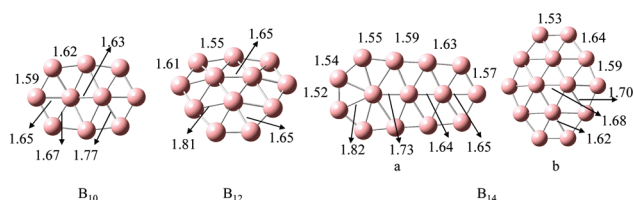(12) Zubarev, D. Y.; Boldyrev, A. I. *J. Comput. Chem.* **2007**, *28*, 251–268.

Figure 1. Geometries of B_{10}, B_{12}, and the two isomers (a and b) of B_{14} along with important bond lengths (Å).

perspective, it should be noted that the B–B single bond distance in B_3H_3 (D_{3h}) is 1.73 Å and experimentally characterized B=B double-bond lengths vary between 1.57 and 1.59 Å. The above distribution of bond lengths indicates that there is strong delocalization of electrons between and within the rings.

Note that B_{12} has 36 valence electrons (12×3), with each boron atom contributing three valence electrons. The manner in which these electrons are arranged can be rationalized as follows. First, 18 electrons are localized along the nine B–B single bonds of the outer B_9 ring. The remaining 18 electrons are divided into 6π electrons, which are delocalized over the entire cluster, and 6σ electrons, which are taken up to make the B_3 ring. The remaining 6 electrons are delocalized between the B_9 and B_3 rings. Thus, the 6π–$6\sigma_{delo}$–$6\sigma_{3\text{-ring}}$ trifurcation can be viewed as giving rise to the triple aromaticity of the B_{12} cluster and is responsible for its unusual stability.

To validate this simple picture, we performed fragment molecular orbital (FMO) calculations.[13] An idealized orbital interaction diagram for the planar B_{12} is presented in Figure 2. Important frontier orbitals of the B_3 and B_9 rings are shown on both sides of the diagram. The B_9 ring has partially filled levels and is unstable on its own. Therefore, interaction with B_3 is necessary for its stabilization. Besides the orbital interactions that constitute three B–B bonds in the B_3 ring ($6\sigma_{3\text{-ring}}$), three radial p-orbital combinations of the B_9 ring ($5e' + 3a_1'$) interact with the corresponding B_3 orbitals ($2a' + 2e'$) to form the σ-bonding combination of $5e'$ and $4a_1'$. This "6-electron" three-orbital interaction between B_9 and B_3 rings is what constitutes a set of aromatic subunits ($6\sigma_{delo}$) of B_{12}. There are three π orbitals ($1e'' + 1a_2''$), which had also been identified earlier, that form another set of the aromatic sextets. Note that the $1e''$ interaction stabilizes the π orbitals below the HOMO level. The additional 6 electrons arising from the three B–B bonds of the B_3 ring complete the triply aromatic nature of B_{12}. It is interesting to note that the LUMO of B_{12} ($2e''$) is a π^* orbital mostly localized on the B_9 ring. The important result from the FMO analysis of B_{12} is that, in addition to the π bonding, there are three molecular orbitals between the B_9 and B_3 rings that contribute to the stabilization of the cluster.

In order to provide further justification to the above distribution of electrons, we performed topological analysis of the electron density using the "Atoms in Molecules" approach.[14] A molecular graph of B_{12} depicting the bond critical points (BCPs) and ring critical points (RCP) is shown in Figure 3. There are a total of 15 BCPs, nine of which are in
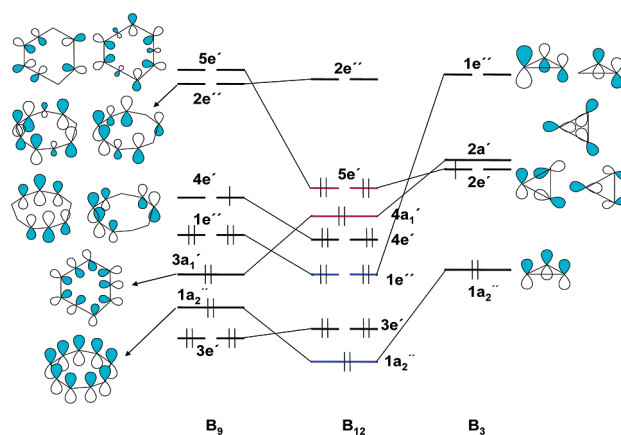
(13) The extended Hückel theory based FMO calculations are done using the *CACAO* program: Mealli, C.; Proserpio, D. M. *J. Chem. Educ.* **1990**, *67*, 399–402.

(14) Bader, R. F. W. *Atoms in Molecules: A Quantum Theory*; Oxford University Press: New York, 1990.

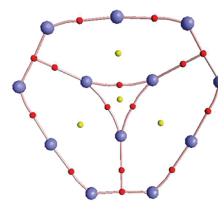**Figure 2.** Idealized orbital interaction diagram for B_{12} (D_{3h}).

Figure 3. Molecular graph of B_{12}. The red dots indicate (3, −1) BCPs, and the yellow dots indicate (3, +1) RCPs.

the outer B_9 ring and three of which are in the B_3 ring. We were able to locate three BCPs, connecting the boron atoms of the inner B_3 ring with the three B–B BCPs of the outer B_9. This corresponds to a conflict structure, in which the boron atoms of the inner B_3 ring are in a competition to link with one of the boron atoms of the outer B_9 ring. Note that, in addition to the RCP located at the center of the B_3 ring, we were also able to find three RCPs between the B_9 and B_3 rings.

It is now easy to explain the stability of B_{13}^+. It has 38 valence electrons and forms a planar (C_{2v}) structure, with 10 boron atoms forming the outer ring (B_{10}) and 3 forming the inner ring (B_3). Partition of the electrons, as was done for B_{12}, can explain the triply aromatic nature of the cluster: Out of 38 valence electrons, 20 are taken up to form the 10 B–B bonds of the B_{10} ring while the remaining 18 electrons are distributed in exactly the same way as that for B_{12}, namely, as $6\pi + 6\sigma_{delo} + 6\sigma_{3\text{-ring}}$ electrons. Not surprisingly, the HOMO and LUMO of B_{13}^+ are the same as those of B_{12}. In other words, both B_{12} and B_{13}^+ have very similar electronic structures (triply aromatic), except that the larger B_{10} ring makes the B_{13}^+ cluster planar. Therefore, the stability of the B_{12} and B_{13}^+ clusters is not just related to the number of π electrons alone but, in fact, to the presence of three distinct aromatic sextets ($4n + 2$), which are unique to these clusters. The H–L gaps in the planar boron clusters depend on the strength of the interaction between the outer and inner rings (such as B_9 and B_3 for B_{12}) and on the overall nature of the π distribution.

What about B_{10} and B_{14}, which have six and eight π electrons, respectively, but have similar H–L gaps ($\sim$1.0 eV)? The orbital pictures of HOMO and LUMO of B_{10}, B_{12}, and B_{14} in Figure 4 provide the answer. As noted above, the H–L gap in B_{12} corresponds to the gap between the σ and π^* levels. This is because the π electrons in B_{12} are more stabilized. On the other hand, the H–L gap in B_{10}
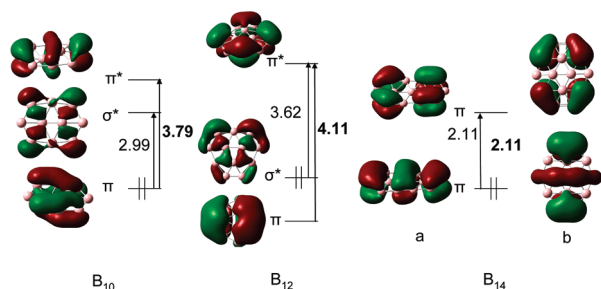
Figure 4. Orbital pictures for B_{10}, B_{12}, and B_{14} (a and b). Gaps of various energy levels are given in electronvolts; values in the bond correspond to $\pi-\pi^*$.

corresponds to the π and σ^* levels. With 8π ($4n$) electrons, B_{14} offers a complementary picture. The $\pi-\pi$ (H−L) gap in B_{14} is the energy difference of otherwise degenerate π orbitals (π orbitals with the same nodes). Not surprisingly, the $\pi-\pi^*$ energy difference is maximum in B_{12} (4.11 eV), followed by

B_{10} (3.79 eV) and B_{14} (2.11 eV). This is consistent with the recent study by Aihara et al., who, using graph theoretical methods, showed that in planar boron clusters the π delocalization reaches a maximum at B_{12}.[15]

In conclusion, we have shown that the unusual but similar electronic structures of B_{12} and B_{13}^+ are due to the existence of multiple $4n + 2$ sextets. The H−L gaps in these planar and quasi-planar boron clusters depend on the nature of the interacting units and not just the π-electron count alone.

Supporting Information Available: Computational details, complete references, and a molecular graph of B_{13}^+. This material is available free of charge via the Internet at http://pubs.acs.org.

(15) Aihara, J.; Kanno, H.; Ishida, T. *J. Am. Chem. Soc.* **2005**, *127*, 13324–13330.